Direct laser writing of symmetry-broken nanocorrals and their applications in SERS spectroscopy

**Jiajia Mu · Jiafang Li · Wuxia Li ·
Shengsheng Sun · Weijie Sun · Changzhi Gu**

Abstract We propose a simple and fast approach to prepare surface-enhanced Raman scattering (SERS) substrates over a large area with high flexibility by using direct laser writing (DLW) technique. The proposal is demonstrated by the direct fabrication of an array and a complex of symmetry-broken nanocorrals with DLW followed by a metal deposition process. SERS measurements show significant SERS enhancement, which can be controlled through engineering the focused "hot spots" by changing the structural parameters. The experimental observations are further confirmed by our simulations with a finite-difference time-domain tool. The studies can be extended to versatile SERS substrates with arbitrary geometries.

Surface-enhanced Raman scattering (SERS) spectroscopy has been widely recognized as a promising and powerful tool in biological, environment and chemical fields [1–3]. To achieve sensitive SERS detection, SERS substrates with high enhancement factors are highly desirable. To this aim, people have created versatile metal nanostructures containing "hot spots" [4, 5], which were randomly distributed in complex metal nanoparticle aggregates or intentionally designed around the tiny features of metal nanostructures such as nanotips and nanogaps [6–13]. At the "hot spots" region, localized plasmonic modes could induce tremendous field enhancement and the resulted SERS

enhancement factor can be as high as 10^{14}–10^{15}. However, the overall SERS enhancement relies on not only the peak enhancement factor at the "hot spots" but also the effective areas of the "hot spots" region. Although the local SERS enhancement factor is promising, the overall SERS enhancement remains very limited if the filling fractions of the "hot spots" areas are small compared with the large substrate areas. Moreover, in some cases, the tiny areas of the "hot spots," for example, the areas between the nanogaps, are not able to accept the detected targets during in situ SERS measurement due to limitations such as heat accumulation and gradient forces. In such a case, generating large-area "hot spots" on a flat substrate is desirable. This can be readily realized by focusing surface plasmon polaritons (SPPs) on a flat substrate. For example, a symmetry-broken nanocorral has recently been employed to generate a pronounced SPP focal spot using linearly polarized illumination. It showed that the focal spot can be well controlled by changing the polarization of the excitation and the geometry of the nanocorrals [14]. However, the nanocorrals (and many other similar structures with SPP focusing functionalities) were generally fabricated by expensive and slow EBL lithography combined with liftoff technique, and the structures have yet been demonstrated in SERS spectroscopy.

Here, we propose and demonstrate a simple, cheap and fast direct laser writing (DLW) of an array and complex of symmetry-broken nanocorrals. After metal deposition, the nanocorrals were directly applied in SERS measurements and showed significant SERS enhancement. Through engineering the focused "hot spots" by changing the structural parameters, the SERS signals were further enhanced, which were confirmed by our simulations with a finite-difference time-domain (FDTD) method. The studies provide a cheap and fast fabrication of SERS substrate over

J. Mu · J. Li (✉) · W. Li · S. Sun · W. Sun · C. Gu (✉)
Beijing National Laboratory for Condensed Matter Physics,
Institute of Physics, Chinese Academy of Sciences,
Beijing 100190, China
e-mail: jiafangli@aphy.iphy.ac.cn

C. Gu
e-mail: czgu@aphy.iphy.ac.cn

a large area with high uniformity, which can be extended to versatile SERS substrates with arbitrary geometries and could be very useful for reproducible, addressable and large-area SERS mapping.

The DLW we used in fabrication is based on two-photon polymerization (2PP) technique [15–19] employed by a commercial fabrication system (Photonic Professional, Nanoscribe GmbH). In fabrication, a 780-nm femtosecond laser beam (with pulse width ~ 120 fs and repetition rate ~ 80 MHz) is focused into a negative photoresist (IP-L, Nanoscribe GmbH) by a high-numerical aperture (NA) oil-immersion objective ($100\times$, NA $= 1.4$, Zeiss), as shown in Fig. 1a. The resolution of DLW is determined by a combination of the optical resolution and the material response during fabrication. The optical resolution is defined by the spatial distribution of absorbed photons, which is mainly governed by the NA of the objective in our case. Figure 1b shows the contour of the intensity square (I^2) of laser in the focal volume, in which only the focal region with photon energy above the 2PP threshold energy of the resist can be polymerized. Therefore, by controlling the laser power during DLW, one can control the size of the polymerized volume in the focus. As shown in Fig. 1c, by exposing the resist with certain dose, ellipsoidal voxels (as the replica of the center focal region) with vertical size ranging from 560 to 1,000 nm can be fabricated. By controlling the central position of the laser focus closely along the top surface of the cover glass, the fabricated voxels can be overlapped with cover glass and stably stand onto its top surface. The width and height of the fabricated features can be less than 100 nm or even thinner [16, 17]. This enables a simple fabrication scheme of metallic nanocorrals. As schematically illustrated in Fig. 1d, a polymeric nanocorral can be firstly fabricated on cover glass by simply scanning the laser spot with certain distance above the top surface of the cover glass. The curvatures of the nanocorrals are sectioned by a serial of separated points in design, and the fabrication is realized by performing point-by-point scanning of the laser spot along the designed routes. Secondly, the sample is developed in 2-propanol for 20 min. Finally, metallic nanocorrals can be obtained by a simple metal deposition process. This three-step fabrication process is very simple and fast. For example, the fabrication of a complex nanocorral (Fig. 2a, containing 10 concentric nanocorrals) and a 100×100 μm^2 nanocorral array (Fig. 2b, containing 1,225 nanocorrals) took less than 10 and 30 min, respectively, with DLW. After the DLW process, a 70-nm-thick Ag film is deposited onto the structures using E-beam evaporation. The three-dimensional nature of the nanocorrals can be well seen in Fig. 2c.

As illustrated in Fig. 1, there are two ways to control the width (d) and height (h) of the fabricated nanocorrals. The first approach is to control the laser power during DLW. As
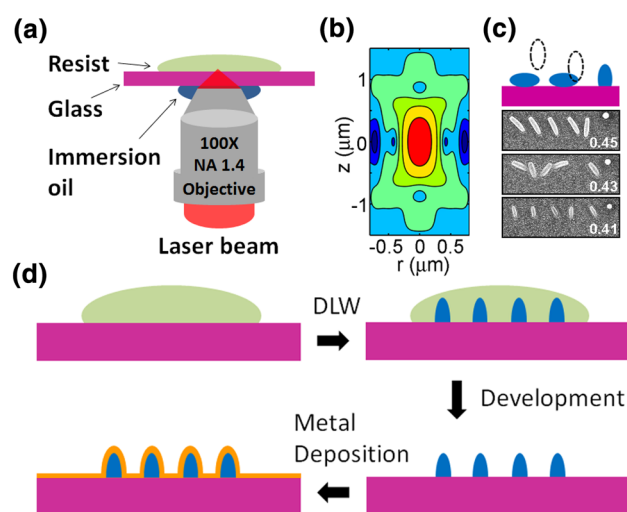

Fig. 1 **a** Schematic diagram for the DLW process. **b** Contour of the normalized intensity square (I^2) in the focal volume of the objective (NA $= 1.4$). **c** Fabrication scheme and top-view SEM images of fabricated replica of the focal volume (named as voxels) under different laser exposure (unit: mJ) as noted. The size of each SEM image is 2×6 μm^2. The sizes of the voxels are $1,000 \times 360$, 800×320 and 560×250 nm^2, respectively, for laser exposure of 4.5, 4.3 and 4.1 mJ. When the scanning height of the laser focus is larger than the size of the voxels, the voxels will lay down after the exposure. When the scanning height is close to the top surface of the cover glass, for example, less than 500 nm, the voxels can well stand onto the substrates, as shown in the top-right corner of each image. This provides the possibility of fabricating corrals in nanoscale. **d** Flowchart for the fabrication of metallic nanocorrals

shown in Fig. 3a–c, by increasing the laser power from 6 to 7, and 8 mW with a constant scanning height, the width of the symmetry-broken nanocorrals (with radius $R_{large} = 1$ μm and $R_{small} = 0.5$ μm) changes from 345 to 397 and 430 nm, while its height is kept unchanged around 500 nm. After the metal deposition process, the nanocorrals are directly immersed into p-thiocresol ethanol solution (with a concentration of $\sim 10^{-5}$ M) for 2 h, rinsed with ethanol to get rid of adsorbed p-thiocresol molecules, and finally dried in air for 20 min, with which the p-thiocresol molecules are attached onto the sample surface with a concentration of $\sim 6.7 \times 10^{-18}$ mol/μm^2. After sample preparations, SERS measurements are performed at room temperature with a Raman microscope (mps 3,000, Laser Quantumn). The excitation laser has a wavelength of 532 nm and excitation power of ~ 1 mW, which is focused onto the nanocorrals from the top by an objective (Olympus, $50\times$, NA $= 0.5$). The diameter of the focus onto the sample is about 1.5 μm. For comparisons, the laser power and accumulation time are kept the same for all SERS measurements. Figure 3d shows the SERS spectra obtained from a layer of p-thiocresol molecules on Ag-coated symmetry-broken nanocorrals with different width. While the planar silver film shows almost no SERS signal, the

Fig. 2 SEM images of fabricated nanocorral complex and nanocorral array. **a** Top-view image of 10 concentric nanocorrals with radius ranging from 0.5 to 10.5 μm. **b** Top-view image of a 35 × 35 symmetry-broken nanocorral array with periodicity of 3 μm. Each nanocrorral consists of two semicorrals with radius $R_{small} = 0.5$ μm and $R_{large} = 1$ μm. *Inset* top-view image of 5 × 5 nanocorrals. **c** Side-view image of single nanocorral from Fig. 2b

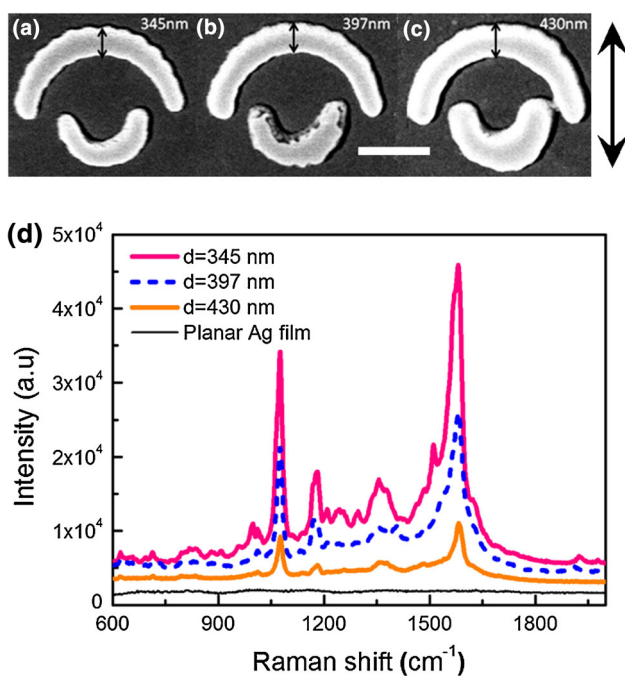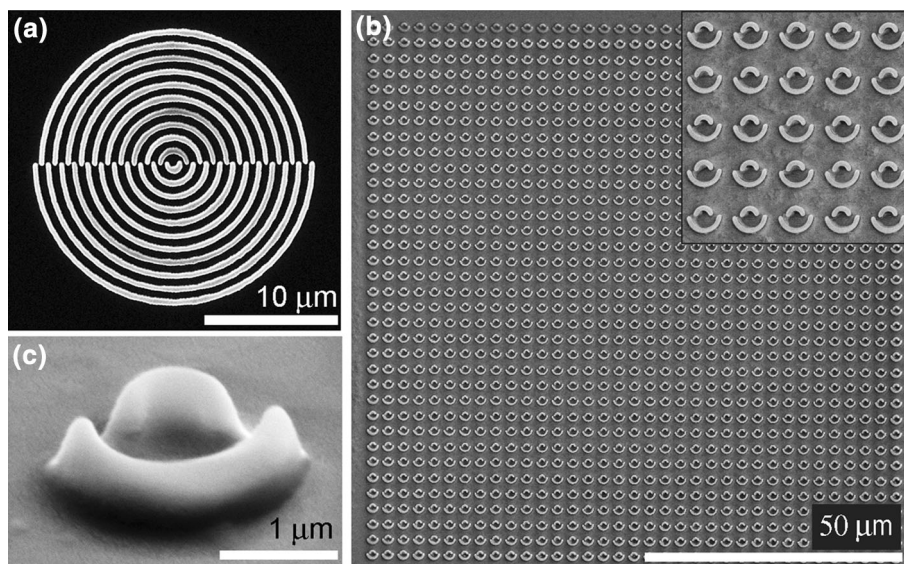**Fig. 3 a–c** Top-view SEM images of symmetry-broken nanocorrals fabricated by DLW under laser power of **a** 6 mW, **b** 7 mW and **c** 8 mW, respectively. The width (*d*) of the nanocorrals is noted in each figure. Each nanocrorral consists of two semicorrals with radius $R_{small} = 0.5$ μm and $R_{large} = 1$ μm. **d** SERS spectra of *p*-thiocresol molecules adsorbed on Ag-coated nanocorral structure with different width as shown in Fig. 3a–c. The SERS measurement from a planar Ag film is also showed as a reference. Excitation wavelength $\lambda = 532$ nm. The excitation polarization direction is indicated by the *arrow* in Fig. 3a–c. The data collection time was set to 6 s

Ag-coated polymeric nanocorrals show significantly enhanced SERS spectra. This is because SPPs are excited and concentrated by the symmetry-broken nanocorrals, which indirectly enhanced the SERS signals through enhancing the local electric field. Moreover, it can be seen that the intensity of the Raman peaks decreased dramatically with the increase in the corral width. This indicates that the width of the nanocorrals affects the excitation and focusing efficiencies of the SPPs, which is consistent with the argument in Ref. [11] that the focal spot can be well controlled by changing the geometry of the nanocorrals.

The other way to control the geometry of the nanocorrals is to change the scanning height of the laser spots while keeping the laser power constantly during the DLW process. Figure 4a shows the measured SERS spectra from nanocorrals with different height, in which the SERS signals are varied as expected. To relatively quantify the experimental results, the Raman enhancement factors (EFs) were calculated by using the following equation given by Yu et al. [20],

$$EF = (I_{SERS}/I_{Ref})(N_{Ref}/N_{SERS})$$

where I_{SERS} and I_{Ref} are the Raman intensities at a certain peak position (1,585 cm^{-1} in this experiment), and N_{Ref} and N_{SERS} are the number of *p*-thiocresol molecules for the reference sample and SERS substrates. The Raman EFs were calculated to be 5×10^5, 3×10^5 and 7×10^4, respectively.

Currently, there are two mechanisms that can be used to explain the SERS enhancement: One is the electromagnetic effect, and the other is the chemical effect. It is well known that the electromagnetic field enhancement accounts for the majority of the SERS signal [21, 22]. To find out why the SERS signals increased with the decrease in the corral height, the electric field (*E*-field) distribution around the nanocorrals is simulated with FDTD method by using a freely available software package (MEEP) [23].

Fig. 4 **a** SERS spectra of *p*-thiocresol molecules adsorbed on Ag-coated nanocorrals structure with different height of (*h*) 300, 500 and 700 nm, respectively. **b–d** Normalized intensity distribution of electric field ($|E|^2/|E_0|^2$) around the Ag nanocorrals with $h = 300$, 500 and 700 nm, respectively, under Gaussian beam excitation at $\lambda = 532$ nm. The two-dimensional (2D) imaging planes are along the top surface of the metal-coated cover glass. *Dashed lines* show the positions of the nanocorrals, and the excitation polarization direction is indicated by the *arrow*. Each nanocrorral consists of two semicorrals with radius $R_{small} = 0.5$ μm and $R_{large} = 1$ μm. The size of each figure is 4×4 μm^2
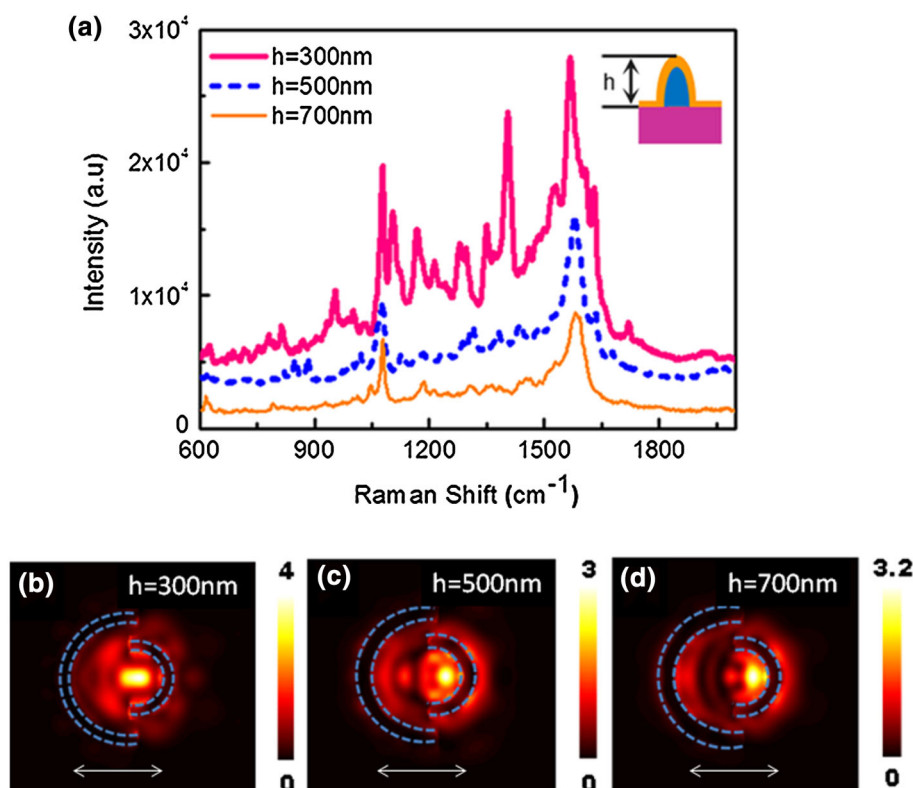
Figure 4b–d plots the normalized intensity distribution of the *E*-field ($|E|^2/|E_0|^2$) around the Ag nanocorrals with a height of 300, 500 and 700 nm, respectively, under Gaussian beam excitation at $\lambda = 532$ nm. As seen from the simulated results, "focal spots" are formed between the left and right semicorrals where the *E*-field intensity is much higher than that at other areas, which could result in a strong Raman signal from locally adsorbed probe molecules. Moreover, both the shape and the size of the "focal spots" are changed with the height of the corrals. Specifically, the position of the "focal spots" moves from the center of the nanocorrals toward the small semicorrals when the corral height increases. Meanwhile, the integrated $|E|^4/|E_0|^4$ value, calculated from FDTD simulations in Figs. 4b–d as a relative indicator of the SERS enhancement, decreases as the corral height increases. For example, when the corral height increases from 300 to 700 nm, the corresponding value of integrated $|E|^4/|E_0|^4$ drops by ~30 % from 3.31 to 2.31. This drop in calculated $|E|^4/|E_0|^4$ corresponds well with the decrease in experimentally measured Raman signals in Fig. 4a, indicating that through engineering the focused "hot spots" by changing the structural parameters of the nanocorrals, the SERS signals can be flexibly controlled.

In conclusion, we have proposed and successfully fabricated symmetry-broken nanocorrals as SERS substrates by DLW and subsequent metal deposition method. By adjusting the laser power and scanning height during DLW, the geometries of the nanocorrals can be well controlled, which provides a flexible approach to modulate the local electric field and therefore control the SERS enhancement factors. Compared with conventional SERS substrates, on the one hand, the proposed substrates can generate large-area "hot spots" and achieve high filed enhancement factors simultaneously on a flat area. On the other hand, compared with the expensive EBL lithography combined with complicated liftoff technique and nanoimprint lithography assisted by expensive and fixed molds, the proposed method is simple, fast, maskless and flexible to directly fabricate two-dimensional and three-dimensional structures with arbitrary geometries [18, 19]. Therefore, taking the symmetry-broken nanocorral as an example, our studies provide a simple, cheap and fast method for the fabrication of SERS substrates with flat detection regions over a large area with variable complexity, which could find potential applications in addressable and large-area SERS mapping.

References

1. S. Nie, S.R. Emory, Probing single molecules and single nanoparticles by surface-enhanced Raman scattering. Science **275**, 1102 (1997)
2. J.A. Dieringer, R.B. Lettan, K.A. Scheidt, R.P. Van Duyne, A frequency domain existence proof of single-molecule surface-enhanced Raman spectroscopy. J. Am. Chem. Soc. **129**, 16249 (2007)
3. M. Fan, A.G. Brolo, Silver nanoparticles self assembly as SERS substrates with near single molecule detection limit. Phys. Chem. Chem. Phys. **11**, 7381 (2009)
4. H. Xu, E.J. Bjerneld, M. Kall, L. Borjesseon, Spectroscopy of single hemoglobin molecules by surface enhanced Raman scattering. Phys. Rev. Lett. **83**, 4357 (1999)
5. J.P. Camden, J.A. Dieringer, Y.M. Wang, D.J. Masiello, L.D. Marks, G.C. Schatz, R.P. Van Duyne, Probing the structure of single-molecule surface-enhanced Raman scattering hot spots. J. Am. Chem. Soc. **130**, 12616 (2008)
6. J.N. Chen, W.S. Yang, K. Dick, K. Deppert, H.Q. Xu, L. Samuelson, H.X. Xu, Tip-enhanced Raman scattering of p-thiocresol molecules on individual gold nanoparticles. Appl. Phys. Lett. **92**, 093110 (2008)
7. H.W. Liu, L. Zhang, X.Y. Lang, Y. Yamaguchi, H. Iwasaki, Y. Inouye, Q.K. Xue, M.W. Chen, Single molecule detection from a large-scale SERS-active Au79Ag21 substrate. Scientific Reports 10 (2011)
8. A. Ahmed, R. Gordon, Single molecule directivity enhanced Raman scattering using nanoantennas. Nano Lett. **12**, 2625 (2012)
9. M.G. Nielsen, A. Pors, O. Albrektsen, S.I. Bozhevolnyi, Efficient absorption of visible radiation by gap plasmon resonators. Opt. Exp. **20**, 13311 (2012)
10. Y.L. Wang, K. Lee, J. Irudayaraj, SERS aptasensor from nanorod-nannoparticle junction for protein detection. Chem. Commun. **46**, 613 (2010)
11. G. Chen, Y. Wang, M.X. Yang, J. Xu, S.J. Goh, M. Pan, H.Y. Chen, Measuring ensemble-averaged surface-enhanced Raman scattering in the hotspots of colloidal nanoparticle dimers and trimers. J. Am. Chem. Soc. **132**, 3644 (2010)
12. C.E. Talley, J.B. Jcakson, C. Oubre, N.K. Grady, C.W. Hollars, S.M. Lane, T.R. Huser, P. Nordlander, N.J. Halas, Surface-enhanced Raman scattering from individual Au nanoparticles and nanoparticle dimer substrates. Nano Lett. **5**, 1569 (2005)
13. L. Liu, Z.H. Han, S.L. He, Novel surface plasmon waveguide for high integration. Opt. Exp. **13**, 6645 (2005)
14. Z.Y. Fang, Q. Peng, W.T. Song, X. Zhu, Plasmonic focusing in symmetry broken nanocorrals. Nano Lett. **11**, 893 (2011)
15. S. Maruo, O. Nakamura, S. Kawata, Three-dimensional microfabrication with two-photon-absorbed photopolymerization. Opt. Lett. **22**, 132 (1997)
16. D. Tan, Y. Li, F. Qi, H. Yang, Q. Gong, X. Dong, X. Duan, Reduction in feature size of two-photon polymerization using scr500. Appl. Phys. Lett. **90**, 071106 (2007)
17. J. Li, B. Jia, M. Gu, Engineering stop gaps of inorganic–organic polymeric 3d woodpile photonic crystals with post-thermal treatment. Opt. Express **16**, 20073 (2008)
18. M.S. Rill, C. Plet, M. Thiel, I. Staude, G. Von Freymann, S. Linden, M. Wegener, Photonic metamaterials by direct laser writing and silver chemical vapour deposition. Nat. Mater. **7**, 543 (2008)
19. M. Thiel, M.S. Rill, G. Freymann, M. Wegener, Three-dimensional bi-chiral photonic crystals. Adv. Mater. **21**, 4680 (2009)
20. H.Z. Yu, H.L. Zhang, Z.F. Liu, Surface-enhanced Raman scattering (SERS) from azobenzene self-assembled "Sandwiches". Langmuir **15**, 16 (1999)
21. K. Kneipp, H. Kneipp, I. Itzkan, R.R. Dasari, M.S. Feld, Surface-enhanced Raman scattering and biophysics. J. Phys. Condens. Matter **14**, R597 (2002)
22. A. Otto, I. Mrozek, H. Grabhorn, W. Akemann, Surface-enhanced Raman scattering. J. Phys. Condens. Matter **4**, 1143 (1992)
23. A.F. Oskooi, D. Roundy, M. Ibanescu, P. Berme, J.D. Joannopoulos, S.G. Johnson, MEEP: a flexible free-software package for electromagnetic simulations by the FDTD method. Comput. Phys. Commun. **181**, 687–702 (2010)